Korean Chem. Eng. Res., 57(4), 547-552 (2019)
https://doi.org/10.9713/kcer.2019.57.4.547
PISSN 0304-128X, EISSN 2233-9558

Electrochemical Performance of High-Voltage $LiMn_{0.8}Fe_{0.2}PO_4$ Cathode with Polyacrylonitrile (PAN)-Based Gel Polymer Electrolyte

O. Hyeon Kwon and Jae-Kwang Kim†

Department of Solar & Energy Engineering, Cheongju University, 298, Daeseong-ro, Cheongwon-gu, Cheongju-si, Chungcheongbuk-do, 28503, Korea
(Received 4 July 2019; Received in revised form 9 July 2019; accepted 11 July 2019)

Abstract – Electrochemical properties of $LiMn_{0.8}Fe_{0.2}PO_4$ cathode were investigated with gel polymer electrolyte (GPE). To access fast and efficient transport of ions and electrons during the charge/discharge process, a pure and well-crystallized $LiMn_{0.8}Fe_{0.2}PO_4$ cathode material was directly synthesized via spray-pyrolysis method. For high operation voltage, polyacrylonitrile (PAN)-based gel polymer electrolyte was then prepared by electrospinning process. The gel polymer electrolyte showed high ionic conductivity of 2.9×10^{-3} S cm^{-1} at 25 °C and good electrochemical stability. Li/GEP/$LiMn_{0.8}Fe_{0.2}PO_4$ cell delivered a discharge capacity of 159 mAh g^{-1} at 0.1 C rate that was close to the theoretical value (170 mAh g^{-1}). The cell allows stable cycle performance (99.3% capacity retention) with discharge capacity of 133.5 mAh g^{-1} for over 300 cycles at 1 C rate and exhibits high rate-capability. PAN-based gel polymer is a suitable electrolyte for application in $LiMn_{0.8}Fe_{0.2}PO_4$/Li batteries with perspective in high energy density and safety.

Key words: $LiMn_{0.8}Fe_{0.2}PO_4$, Polyacrylonitrile, High potential, Electrochemical performance, Lithium ion battery

1. Introduction

Cathode materials are one of the most important components of lithium ion batteries [1-3]. For lithium ion batteries, $LiMPO_4$ (M = Fe, Mn, Co, Ni ...) compounds having an olivine structure have attracted great attention as cathode materials because of stable crystal structure upon electrochemical reaction with Li^+ [4]. Among the others, $LiFePO_4$ is recognized as one of the most promising material for applications in large-scale energy storage due to its good stability, non-toxicity, low cost and especially high theoretical capacity (~ 170 mAh g^{-1}) [5,6]. However, $LiFePO_4$ has issues of poor conductivity (both ionic and electronic), which generally causes the loss of capacity at high charge-discharge current density [7,8]. At the same time, $LiMnPO_4$ is also attracting attention since its properties are similar to those of $LiFePO_4$. Furthermore, $LiMnPO_4$ has higher energy density than $LiFePO_4$ (3.4 V vs. Li / Li^+) thanks to the higher potential of Li^+ storage: 4.1 V vs. Li / Li^+ [9-14]. However, also, the $LiMnPO_4$ exhibits low electronic conductivity (<10^{-10} S cm^{-1}), a slow lithium ion diffusion (<10^{-16} cm^2 S^{-1}) compared to the $LiFePO_4$ (1.8×10^{-9} S cm^{-1}), and thus low specific discharge capacity and rate performance [15]. Moreover, it shows the Jahn-Teller effect caused by limits of lattice distortions since the Mn^{3+} at charged state destroys the structural stability in the electrochemical activity, which results in poor capacity retention [16,17]. To overcome these problems, Mn site can be substituted by Fe, providing advantages of improved stability of $LiMnPO_4$ by better electron conductivity and weakening Jahn-Teller distortion of Mn^{3+} ion by forming $LiMn_xFe_{1-x}PO_4$ (LMFP) solid solution [18]. Recently, many studies have been carried out on the synthesis, phase structure, reaction mechanism and performance improvement of LMFP [19-23]. LMFP with $x < 0.4$ has often been employed in lithium ion batteries, while LMFP with $x > 0.75$ and Mn-rich phases has not been investigated due to the poor performance with commercial liquid electrolyte (EC:DMC 1M $LiPF_6$) [24,25].

Polyacrylonitrile (PAN)-based gel polymers are perspective electrolytes for addressing this problem [26,27]. The PAN has additional characteristics of low flammability, good processability, oxidative degradation and electrochemical stability. It contains a nitrile group with strong polarity that prevents alignment of the polymer chains during electrospinning, allowing the production of flexible membranes with excellent mechanical strength. Furthermore, PAN gel polymer electrolytes exhibited interesting properties such as high ionic conductivity, high oxidation stability > 4.7 V, improved thermal stability, good electrolyte absorption and compatibility with lithium metal anode [28]. Indeed, it has been proved to minimize the dendrite growth during charge/discharge [29].

In this study, PAN-based gel polymer electrolyte is used together with $LiMn_{0.8}Fe_{0.2}PO_4$ (LMFP) cathode. The PAN membrane was prepared by electrospinning and showed high ionic conductivity and electrochemical oxidation stability. By coupling the PAN-based electrolyte with LMFP cathode in Li-half cells we demonstrate a high discharge capacity, excellent cycle performance and good rate-capability.

2. Experimental

2-1. $LiMn_{0.8}Fe_{0.2}PO_4$ synthesis

All chemicals (99%) for LMFP synthesis were obtained from

† To whom correspondence should be addressed.
E-mail: jaekwang@cju.ac.kr

Aldrich. Stoichiometric quantities of LiCl, $FeCl_2 \cdot 4H_2O$, Mn $(COOCH_3)_2 \cdot 4H_2O$ and H_3PO_4 were dissolved in distilled water, and homogeneous precursor solution with a concentration of 0.05 M was gained. HCl was added to control the pH of the precursor solution. The synthesis started with the atomization of the precursor solution, which was done by a fluid-nozzle utilizing nitrogen gas. Thus, a fine aerosol with an average droplet size below 30 μm was created. The aerosol was transported into the reaction chamber, which consisted of a quartz tube placed in a furnace with three-step heating zones. For the $LiMn_{0.8}F_{0.2}PO_4$ synthesis the first heat zone was held at approximately 70 °C to preheat the aerosol. The second and third heat zones were kept at 800 °C. The product was collected by sedimentation in a round bottom flask which was held at a temperature of 120 °C to avoid the condensation of vaporized water.

2-2. Gel-polymer electrolyte (GPE) preparation

Electrospinning process was employed for the preparation of PAN-based gel polymer electrolyte. In particular, the colloidal solution for electrospinning was prepared by dissolving 0.6 g of PAN (Mw: 200,000, Polysciences, Inc) in 10mL of dimethylformamide (DMF, Samchun, 99.5%). The prepared solution was filled in a plastic syringe equipped with a 21-gauge stainless steel nozzle. The filled solution was ejected at a flow 0.5 mL h^{-1}, the rotation speed of the drum collector was 200 rpm, the applied voltage between the collector and the syringe tip was maintained at 18 kV. The PAN nanofibers obtained after electrospinning were dried in a vacuum oven at 80 °C for 12 h. Finally, the gel polymer electrolyte was prepared by soaking the electrospun PAN matrix for 3 min in a solution of 1 M $LiPF_6$ in ethylene carbonate (EC)/dimethyl carbonate (DMC) (1:1 by vol.) [PanaX. Etec Co.].

2-3. Characterization Techniques

The morphology and three-dimensional surface structure were investigated through field-emission scanning electron microscopy (FE-SEM, JSM-7610F, JEOL). An energy dispersive x-ray spectrometer (EDS, JSM-7610F, JEOL) analysis was performed to identify the overall elemental distribution of the FE-SEM image by color difference. Phase was analyzed by X-ray diffractometry (XRD, SmartLab3, Rigaku) using Cu-radiation. The electrochemical property of the LMFP was analyzed by building coin cells using PAN-based gel polymer as both electrolyte and separator. For half-cell, lithium metal was used as counter electrode. The gel polymer electrolyte was used by soaking PAN matrix in a solution of 1 M $LiPF_6$ dissolved in ethylene carbonate (EC)/dimethyl carbonate (DMC) (1:1 by volume). The cathode was prepared by mixing LMFP, carbon black and poly vinylidene fluoride (PVDF) in a weight ratio of 85:8:7. Cyclic voltammetry (CV) measurements of the Li/GPE/LMFP cells were performed at a scan rate of 0.1 mV s^{-1} over 2.5~4.4 V. The charge/discharge characteristics of samples were measured at various current densities in the voltage range of 2.5~4.4 V. Electrochemical performance was tested using an automatic galvanostatic charge-discharge unit, WBCS3000 battery cycler. The area of the cathode was 0.785 cm^2 with a mass loading 2.6 mg. Rate performance was investigated at different current densities ranging from 0.1 C to 5.0 C (1C = 170 mA).

3. Results and Discussion

Fig. 1 shows the X-ray diffraction (XRD) patterns of the LMFP: LMFP has an olivine structure corresponding to standard $LiMnPO_4$ (JCPDS No.74-0375) and $LiFePO_4$ (JCPDS No.40-1499). The crystalline parameters of LMFP are reported in Table 1. These values range between $LiFePO_4$ and $LiMnPO_4$. Refined unit cell parameters were calculated from XRD patterns as a = 10.41, b = 6.07, and c = 4.731, corresponding to orthorhombic unit cell, similar to $LiFePO_4$ and $LiMnPO_4$ compounds. There was no evidence of crystalline and amorphous carbon since there was only very small amount of carbon and thin layer on LMFP. No impurity phases from the entire diffraction patterns of LMFP were detected, while quite narrow peaks indicated well-crystallized structure. Elemental analysis was used to determine the amount of carbon, i.e., around 2% for all samples.

The morphology of the sample was observed by field-emission scanning electron microscopy (FE-SEM) while the element distribution by using the FE-SEM energy dispersive x-rays spectroscopy (EDS). The FE-SEM images, Fig. 2(a), show that all particles have spherical morphology with a uniform fine-grained microstructure and particle size in the range of 2~3 μm. The LMFP microspheres are composed of smaller primary particles with sizes of about 80 nm. The microspherical morphology is necessary to improve the tap density of the electrode powder because they can be better packed together [30-32]. In fact, the LMFP electrode has high tap density of 1.25 g cm^{-3}, which is higher

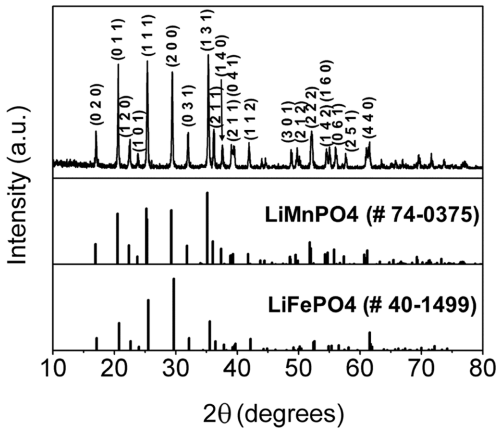

Fig. 1. XRD patterns of standard $LiFePO_4$, $LiMnPO_4$ and prepared $LiMn_{0.8}Fe_{0.2}PO_4$.

Table 1. Unit cell parameters of $LiFePO_4$, $LiMnPO_4$ and prepared $LiMn_{0.8}Fe_{0.2}PO_4$

Sample	Cell parameter (Å)		
	a	b	c
LMFP	10.41	6.07	4.731
$LiMnPO_4$	10.46	6.10	4.744
$LiFePO_4$	10.35	6.02	4.704

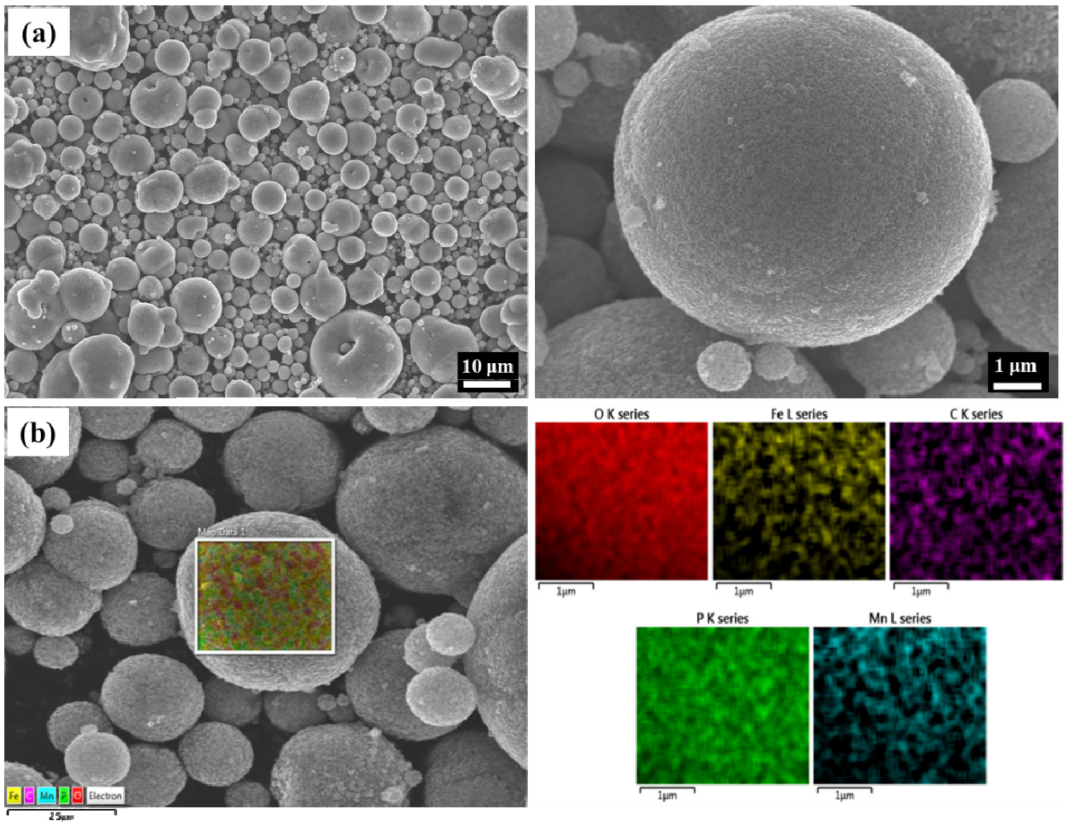

Fig. 2. SEM images (a) and EDX images (b) of LMFP microspherical powders.

than typical tap densities of nanoparticles (0.3~0.8 g cm^{-3}) [33]. The high tap density improves the volumetric capacity. Fig. 2(b) shows the SEM images of LMFP and the corresponding EDS element mapping of Fe, O, C, P, and Mn. The distribution of elements, Fe, Mn, O, and P is very uniform in the particles. Furthermore, the distribution of C element is also homogeneous, confirming a uniform layer on the surface of LMFP microspheres.

The PAN matrix is fabricated through electrospinning. Fig. 3(a)

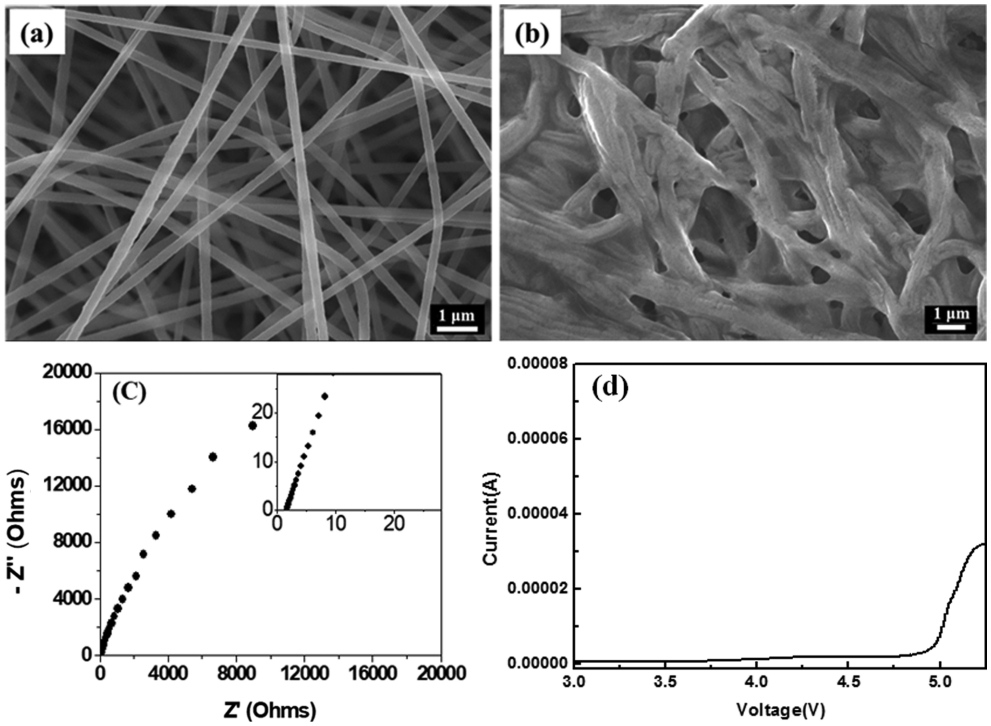

Fig. 3. SEM images of electrospun PAN membrane (a) and gel polymer electrolyte (b), electrochemical impedance spectroscopy (c) and LSV (d) of gel polymer electrolyte.

shows FE-SEM images of the electrospun PAN nanofibers. The fibers display homogeneously distributed diameters in the range 200 to 350 nm and a relatively smooth and straight surface structure. They are made up of a network of interlaid fibers, and the interconnection of the fibers imparts sufficient mechanical strength to the membrane for safe handling. Fig. 3(b) shows FE-SEM images of the PAN membrane after soaking in the electrolyte. Membranes that absorb large amounts of liquid electrolyte appeared to have high porosity and partial gelation of PAN membranes. The gelation of porous PAN membranes is attributed to the affinity with the electrolyte solution for the presence of polar functional groups present in the PAN [34]. The ionic conductivity of PAN-based gel polymer electrolytes is calculated from $\sigma = L/(R_bA)$. (where R_b is the bulk resistance of the gel electrolyte obtained from the complex impedance measurement, L and A are the thickness and area of the sample membrane disk, respectively). R_b could be obtained from the real axial intercept of the complex impedance at the high frequency end of the Nyquist plot [35,36]. Fig. 3(c) shows the complex impedance spectra of the PAN-based gel polymer electrolyte at room temperature. The ionic conductivity is of 2.9×10^{-3} S/cm. Fig. 3(d) shows the linear sweep voltammograms (LSV) of PAN-based gel polymer electrolyte. The gel polymer electrolyte has high electrochemical oxidation stability up to 4.9 V. From the electrochemical window results, it is established that PAN-based gel polymer electrolyte is acceptable with high voltage intercalation compound cathodes like LMFP.

Fig. 4 displays the electrolyte uptakes of the PAN membrane with time. The membrane reached its respective maximum amounts within 2 min. The PAN matrix exhibited high absorption (~370%) because it consists of fibers with pores. The liquid electrolyte is trapped in the spaces formed between the polymer fibers, resulting in the absorption of higher amount of liquid electrolyte. The high uptake of liquid electrolyte in gel phase is beneficial to achieving high electrochemical properties.

Fig. 5 reports the cyclic voltammetry (CV) of $LiFePO_4$ and LMFP in the voltage range between 2.5 and 4.4 V. The CV of LMFP shows the redox activity of the Mn^{2+}/Mn^{3+} and Fe^{2+}/Fe^{3+} couples (peak potentials

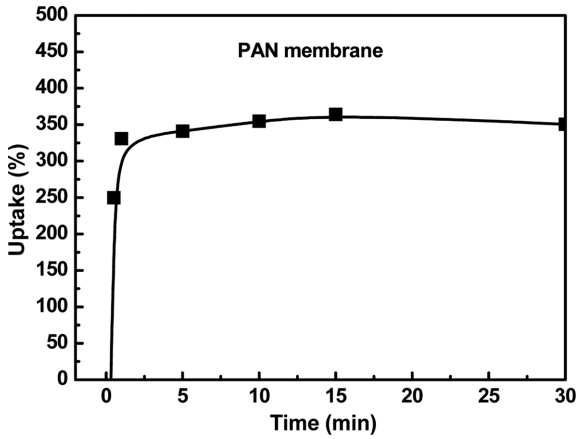

Fig. 4. Uptake analysis of electrospun PAN membrane.

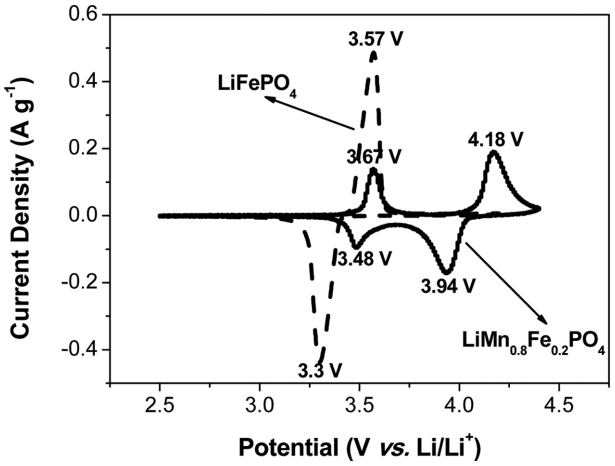

Fig. 5. Cyclic voltammetry of $LiFePO_4$ and LMFP cells.

at about 4.18/3.94 V and 3.67/3.48 V, respectively) at the expected ratio of the charges involved (4:1). On the comparison with $LiFePO_4$, the oxidation peak potential of Fe_2^+/Fe_3^+ shifts slightly to lower potential (from 3.57 V to 3.67 V), while reduction peak to higher (from 3.3 V to 3.48 V). This means that the Fe redox pair of LMFP is more reversible than in $LiFePO_4$. It is clear that the presence of Mn^{2+} is affected by the electrochemical reaction of the Fe.

Fig. 6(a) shows the discharge-charge voltage profiles of Li/GPE/LMFP cell from 1st to 5th cycles, using a current of 0.1C (17 mA g^{-1}). The discharge capacity reaches 159 mAh g^{-1} in the 1st cycle and 159.7 mAh g^{-1} and 160.1 mAh g^{-1} in the 2nd and 5th cycles, respectively, with a low irreversible capacity in 1st cycle. The voltage profiles highlight two distinct plateaus at ~3.5 and ~4.0 V, respectively, associated with the Fe^{2+} / Fe^{3+} and Mn^{2+} / Mn^{3+} redox couples. A slope profile is highlighted in the Fe^{2+} / Fe^{3+} reaction region, which is related to the solid solution phase transformation mechanism [37,38]. A broad flat plateau around 4 V shows a two-phase equilibrium between the phase of fully lithiated $LiMnPO_4$ and the phase of fully delithiated $MnPO_4$ [24]. The discharge capacity and operation potential is higher than the reported Li/$LiFePO_4$ and $LiMnPO_4$ gel polymer cells [22,28,29]. The rate performance of Li/GPE/LMFP cells is reported in Fig. 6(b) at different current rates within 10 cycles. The reversible discharge capacity remains 147.3 mAh g^{-1} at 0.5 C and 84.8 mAh g^{-1} at the 5 C rate without any capacity fade for over 70 cycles. The LMFP cell shows good capacity stability at every rate and the cell recovers almost the full discharge capacity at initial cycle when the current is lowered back to 0.1 C after 50 cycles at different rates, which means that the cell has good rate capability. The prolonged cycling performance of Li/GPE/LMFP cell at 1.0 C rate was also evaluated. As shown in Fig. 6(c), the discharge capacity of LMFP remains stable at 133.5 mAh g^{-1} for over 300 cycles. The discharge capacity retention rate measured in the first cycle was 99.3%, while Coulombic efficiency at the first cycle was 98%, while is higher than 99% from 2nd until the 300th cycle, with no capacity loss.

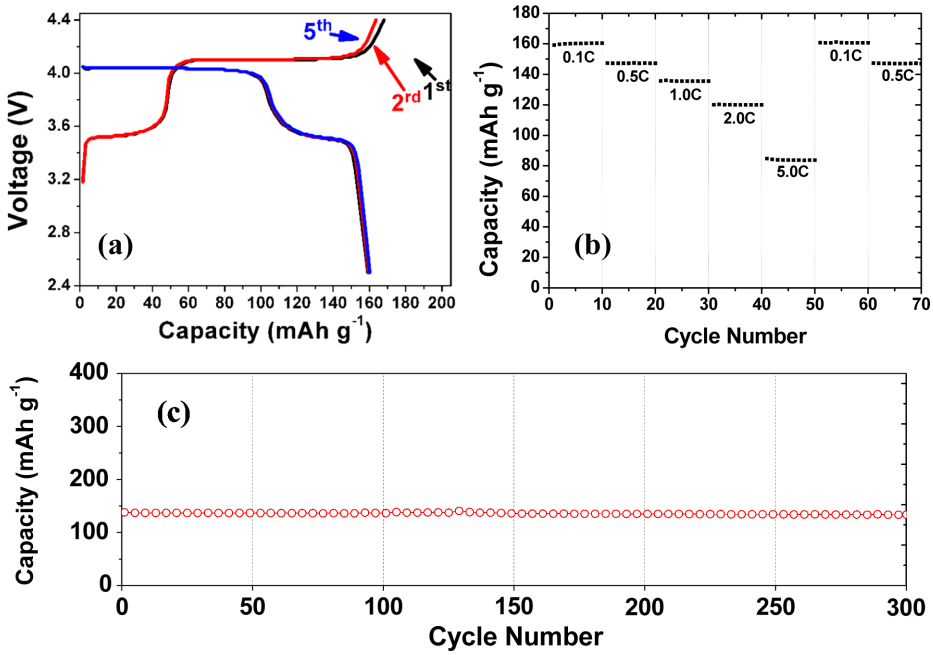

Fig. 6. Charge-discharge profiles (a), rate-capability (b) and cycle performance Li/GPE/LMFP cells.

4. Conclusions

The electrochemical performance of high voltage $Li/LiMn_{0.8}Fe_{0.2}PO_4$ cell was evaluated using a PAN-based gel polymer electrolyte. The $LiMn_{0.8}Fe_{0.2}PO_4$ synthesized by spray-pyrolysis method showed well-crystallized structure with microspherical morphology. The electrospun PAN-based gel polymer electrolyte demonstrated high ionic conductivity, of about 2.9×10^{-3} S cm^{-1} at 25 °C, and high electrochemical oxidation stability. The PAN polymer electrolyte coupled with $LiMn_{0.8}Fe_{0.2}PO_4$ in Li-half cells exhibited high and excellent cycling performance with initial discharge capacity of 159.0, 147.3, 134.8 and 84.8 mAh g^{-1} at 0.1, 0.5, 1 and 5 C-rates, respectively. In addition, even after 300 cycles at the high current rate of 1 C, a discharge capacity of 133.5 mAh g^{-1} was obtained with high retention and low capacity loss of only 0.004% per cycle. The results here reported demonstrate that PAN-based gel polymers prepared through electrospinning techniques are suitable electrolytes for application in $Li/LiMn_{0.8}Fe_{0.2}PO_4$ cells.

Acknowledgement

This work was supported by the research grant of Cheongju University (2017.09.01.~2019.08.31.).

References

1. Jeon, D. M., Na, B. K. and Rhee, Y. Woo., "Electrochemical Characteristics of Si/PC/CNF/PC Composite for Anode Material of Lithium ion Battery," *Korean Chem. Eng. Res.*, **56**(6), 798-803(2018).
2. Fan, Z. Yu., Jin, E. M. and Jeong, S. M., "Enhanced Electrochemical Properties of NCA Cathode Materials for Lithium Ion Battery by Doping Effect," *Korean Chem. Eng. Res.*, **55**(6), 861-867(2017).
3. Lim, J.-E. and Kim, J.-K., "Optimization of Electrolyte and Carbon Conductor for Dilithium Terephthalate Organic Batteries," *Korean J. Chem. Eng.*, **35**(12), 2464-2467(2018).
4. Chung, S. Y., Bloking, J. T. and Chiang, Y. M., "Electronically Conductive Phospho-olivines as Lithium Storage Electrodes," *Nature* Materials, **1**(2), 123-128(2002).
5. Huang, Y. H. and Goodenough, J. B., "High-rate $LiFePO_4$ Lithium Rechargeable Battery Promoted by Electrochemically Active Polymers," *Chemistry of Materials*, **20**(23), 7237-7241(2008).
6. Kang, B. and Ceder, G., "Battery Materials for Ultrafast Charging and Discharging," *Nature*, **458**(7235), 190-193(2009).
7. Tarascon, J. M. and Armand, M., "Issues and Challenges Facing Rechargeable Lithium Batteries," *Nature*, **414**, 359-367(2001).
8. Zane, D., Carewska, M., Scaccia, S., Cardellini, F. and Prosini, P. P., "Factor Affecting Rate Performance of Undoped $LiFePO_4$," *Electrochimica Acta*, **49**(25), 4259-4271(2004).
9. Wang, L., Zhou, F. and Ceder, G., "Ab Initio Study of the Surface Properties and Nanoscale Effects of $LiMnPO_4$," *Electrochemical and Solid-State Letters*, **11**(6), A94-A96(2008).
10. Drezen, T., Kwon, N. H., Bowen, P., Teerlinck, I., Isono, M. and Exnar, I., "Effect of Particle Size on $LiMnPO_4$ Cathodes," *J. Power Sources*, **174**(2), 949-953(2007).
11. Martha, S. K., Markovsky, B., Grinblat, J., Gofer, Y., Haik, O., Zinigrad, E. and Exnar, I., "$LiMnPO_4$ as an Advanced Cathode Material for Rechargeable Lithium Batteries," *J. Electrochemical Society*, **156**(7), A541-A552(2009).
12. Choi, D., Wang, D., Bae, I. T., Xiao, J., Nie, Z., Wang, W. and Yang, Z., "$LiMnPO_4$ Nanoplate Grown via Solid-State Reaction in Molten Hydrocarbon for Li-ion Battery Cathode," *Nano Letters*, **10**(8), 2799-2805(2010).
13. Bakenov, Z. and Taniguchi, I., "Physical and Electrochemical Properties of $LiMnPO_4$/C Composite Cathode Prepared with Differ-

ent Conductive Carbons," *J. Power Sources*, **195**(21), 7445-7451 (2010).
14. Kang, B. and Ceder, G., "Electrochemical Performance of $LiMnPO_4$ Synthesized with Off-Stoichiometry," *J. Electrochemical Society*, **157**(7), A808-A811(2010).
15. Yonemura, M., Yamada, A., Takei, Y., Sonoyama, N. and Kanno, R., "Comparative Kinetic Study of Olivine Li_xMPO_4 (M = Fe, Mn)," *J. Electrochemical Society*, **151**(9), A1352-A1356(2004).
16. Zhou, F., Cococcioni, M., Marianetti, C. A., Morgan, D. and Ceder, G., "First-Principles Prediction of Redox Potentials in Transition-metal Compounds with LDA+ U," *Physical Review B*, **70**(23), 235121(2004).
17. Yamada, A., Hosoya, M., Chung, S. C., Kudo, Y., Hinokuma, K., Liu, K. Y. and Nishi, Y., "Olivine-type Cathodes: Achievements and Problems," *J. Power Sources*, **119-121**, 232-238(2003).
18. Yan, S. Y., Wang, C. Y., Gu, R. M., Sun, S. and Li, M. W., "Synergetic Fe Substitution and Carbon Connection in $LiMn_{1-x}FexPO_4$/C Cathode Materials for Enhanced Electrochemical Performances," *J. Alloys and Compounds*, **628**, 471-479(2015).
19. Li, G., Azuma, H. and Tohda, M., "Optimized $LiMn_yFe_{1-y}PO_4$ as the Cathode for Lithium Batteries," *J. Electrochemical Society*, **149**(6), A743-A747(2002).
20. Mi, C. H., Zhang, X. G., Zhao, X. B. and Li, H. L., "Synthesis and Performance of $LiMn_{0.6}Fe_{0.4}PO_4$/nano-carbon Webs Composite Cathode," *Materials Science and Engineering: B*, **129**(1-3), 8-13(2006).
21. Hong, J., Wang, F., Wang, X. and Graetz, J., "$LiFexMn_{1-x}PO_4$: A Cathode for Lithium-ion Batteries," *J. Power Sources*, **196**(7), 3659-3663(2011).
22. Hu, C., Yi, H., Fang, H., Yang, B., Yao, Y., Ma, W. and Dai, Y., "Improving the Electrochemical Activity of $LiMnPO_4$ via Mn-site Co-substitution with Fe and Mg," *Electrochemistry Communications*, **12**(12), 1784-1787(2010).
23. Kim, J. K., Hwang, G. C., Kim, S. H. and Ahn, J. H., "Comparison of the Structural and Electrochemical Properties of $LiMn_{0.4}Fe_{0.6}PO_4$ Cathode Materials with Different Synthetic Routes," *J. Industrial and Engineering Chemistry*, **66**, 94-99(2018).
24. Yamada, A., Kudo, Y. and Liu, K. Y., "Phase Diagram of $Lix(Mn_yFe_{1-y})PO_4$ ($0 \leqslant x, y \leqslant 1$)," *J. Electrochemical Society*, **148**(10), A1153-A1158(2001).
25. Yamada, A. and Chung, S. C., "Crystal Chemistry of the Olivine-Type Li $(Mn_yFe_{1-y})PO_4$ and $(Mn_yFe_{1-y})PO_4$ as Possible 4 V Cathode Materials for Lithium Batteries," *J. Electrochemical Society*, **148**(8), A960-A967(2001).
26. Abbrent, S., Plestil, J., Hlavata, D., Lindgren, J., Tegenfeldt, J. and Wendsjö, Å. "Crystallinity and Morphology of PVdF-HFP-based Gel Electrolytes," *Polymer*, **42**(4), 1407-1416(2001).
27. Huang, B., Wang, Z., Chen, L., Xue, R. and Wang, F., "The Mechanism of Lithium Ion Transport in Polyacrylonitrile-based Polymer Electrolytes," *Solid State Ionics*, **91**(3-4), 279-284(1996).
28. Raghavan, P., Manuel, J., Zhao, X., Kim, D. S., Ahn, J. H. and Nah, C., "Preparation and Electrochemical Characterization of Gel Polymer Electrolyte based on Electrospun Polyacrylonitrile Nonwoven Membranes for Lithium Batteries," *J. Power Sources*, **196**(16), 6742-6749(2011).
29. Tsutsumi, H., Matsuo, A., Takase, K., Doi, S., Hisanaga, A., Onimura, K. and Oishi, T., "Conductivity Enhancement of Polyacrylonitrile-based Electrolytes by Addition of Cascade Nitrile Compounds," *J. Power Sources*, **90**(1), 33-38(2000).
30. Jo, M. S., Ghosh,S., Jeong, S. M., Kang, Y. C. and Cho, J. S., "Coral-Like Yolk-Shell-Structured Nickel Oxide/Carbon Composite Microspheres for High-Performance Li-Ion Storage Anodes," *Nano-Micro Lett*., **11**(1), 1-18(2019).
31. Oh, S. H., Kim, J. K., Kang, Y. C. and Cho, J. S., "Three-Dimensionally Ordered Mesoporous Multicomponent (Ni, Mo) Metal Oxide/N-doped Carbon Composite with Superior Li-Ion Storage Performance," *Nanoscale*, **10**(39), 18734-18741(2018).
32. Ko, H. S., Park, H. W., Kim, G. J. and Lee, J. D., "Electrochemical Characteristics of Lithium-Excess Cathode Material ($Li_{1+x}Ni_{0.9}Co_{0.05}Ti_{0.05}O_2$) for Lithium-Ion Batteries," *Korean J. Chem. Eng*., **36**(4), 620-624(2019).
33. Wang, Y., He, P. and Zhou, H., "Olivine $LiFePO_4$: Development and Future," *Energy Environ. Sci*., **4**(3), 805-817(2011).
34. Raghavan, P., Choi, J. W., Ahn, J. H., Cheruvally, G., Chauhan, G. S., Ahn, H. J. and Nah, C., "Novel Electrospun Poly(vinylidene fluoride-co-hexafluoropropylene)-in situ SiO_2 Composite Membrane-based Polymer Electrolyte for Lithium Batteries," *J. Power Sources*, **184**(2), 437-443(2008).
35. Min, H. S., Ko, J. M. and Kim, D. W., "Preparation and Characterization of Porous Polyacrylonitrile Membranes for Lithium-ion Polymer Batteries," *J. Power Sources*, **119**, 469-472(2003).
36. Abraham, K. M., Jiang, Z. and Carroll, B., "Highly Conductive PEO-like Polymer Electrolytes," *Chemistry of Materials*, **9**(9), 1978-1988(1997).
37. Watanabe, M., Sanui, K., Ogata, N., Kobayashi, T. and Ohtaki, Z., "Ionic Conductivity and Mobility in Network Polymers from Poly(propylene oxide) Containing Lithium Perchlorate," *J. Applied Physics*, **57**(1), 123-128(1985).
38. Roberts, M. R., Vitins, G., Denuault, G. and Owen, J. R., "High Throughput Electrochemical Observation of Structural Phase Changes in $LiFe_{1-x}Mn_xPO_4$ during Charge and Discharge," *J. Electrochemical Society*, **157**(4), A381-A386(2010).